Talanta 127 (2014) 269–275

Contents lists available at ScienceDirect

Talanta

journal homepage: www.elsevier.com/locate/talanta

Polystyrene/Ag nanoparticles as dynamic surface-enhanced Raman spectroscopy substrates for sensitive detection of organophosphorus pesticides

Pan Li [a], Ronglu Dong [a], Yiping Wu [b], Honglin Liu [b], Lingtao Kong [a,b,*], Liangbao Yang [a,b,*]

[a] Department of Chemistry, University of Science & Technology of China, Hefei, Anhui 230026, China
[b] Institute of Intelligent Machines, Chinese Academy of Sciences, Hefei 230031, China

ARTICLE INFO

Article history:
Received 13 January 2014
Received in revised form
23 March 2014
Accepted 29 March 2014
Available online 12 April 2014

Keywords:
Dynamic
SERS
Organophosphorus pesticides
Quantitative analysis

ABSTRACT

We report the use of Polystyrene/Ag (PS/Ag) nanoparticles as dynamic surface-enhanced Raman spectroscopy (dynamic-SERS) substrates for sensitive detection of low levels of organophosphorus pesticides. The PS particles clearly observed using Raman microscopy provide the masterplate for in situ growth of Ag NPs, leading to multiple active sites for SERS measurements. Besides obtaining the fingerprints of target molecules and recording time-resolved Raman spectra, this dynamic-SERS method can be used as an ultra-sensitive analytical technique which can enhance 1–2 orders of magnitude the signals of analytes in comparison to that of the traditional methods. On the other hand, importantly, it shows much better correlations between concentration and intensity than does the conventional SERS technique so that it can build the foundation for quantitative analysis of analytes. The as-prepared individual PS/Ag nanoparticle has been demonstrated for the sensitive detection of organophosphorus paraoxon and sumithion. SERS spectra are acquired at different concentrations of each pesticide and linear calibration curves are obtained by monitoring the strongest intensity value of bands arising from stronger stretching mode as a function of analyte concentration. The limits of detection and limits of quantitation are reported for two pesticides. The limit of detection for paraoxon is 96 nM (0.026 ppm) and for sumithion is 34 nM (0.011 ppm). The limits of quantitation are 152 nM (0.042 ppm) and 57 nM (0.016 ppm) for paraoxon and sumithion, respectively. It can be seen that these two organophosphorus pesticides can be detected in the low nM range based on this dynamic-SERS analytical method. Also, in the real sample experiments of paraoxon and sumithion, the results confirm that this dynamic-SERS technique would have potential applicability for quantitative analysis with slight interference.

1. Introduction

Organic pollutants such as aromatic organic dyes resulting from industrial emissions and agricultural chemical products resulting from the manufacturing of insecticides are present in river, lake or soil [1–3], where these pollutants are the important environmental issues and have a serious threat to ecosystems as well as human health. Therefore, it is of importance to develop a sensitive and convenient analytical technique to be applied for the detection of trace amounts of organic pollutants. Also, quantitative determination of pollutants is necessary in order to mitigate or monitor potential human exposure via pesticide residues left on inadequately washed food items as well as groundwater contamination from agricultural runoff. However, a few traditional in situ analytical methods can achieve the purpose entirely because of the lower sensitivity or extensive sample preparation. SERS has been widely used as a powerful analytical technique with potential lower detection limits. However, SERS is not only dictated by such low detection limits, but also by the complete information that it can provide, since the spectra contain all the vibrational information of the analytes, and its applications, which can be carried out at environment conditions without considering physical states of samples and with no need of sophisticated analytical preparations [4]. Moreover, SERS signals are less sensitive to photobleaching than fluorescence signals, thus permit signals collection of longer times and improve signal average and stability [5–8]. In addition, SERS has been proved to be a promising tool for nondestructive, ultra-fast and sensitive detection even down to the single molecular level [9–11]. It also has been used for theoretical

* Corresponding authors at: Department of Chemistry, University of Science & Technology of China, Hefei, Anhui 230026, China.
Tel.: +86 551 5592385; fax: +86 551 5592420.
E-mail addresses: ltkong@iim.ac.cn (L. Kong), lbyang@iim.ac.cn (L. Yang).

http://dx.doi.org/10.1016/j.talanta.2014.03.075
0039-9140/

investigations of chemical structures and dynamic interface behavior by providing time-resolved "fingerprint" information [12–14].

In principle, the signal intensity observed in spontaneous SERS measurements is proportional to the concentration in the probed volume, so it should be possible to make a direct calibration plot of the absolute intensity of the Raman band against concentration. However, it is well-known that accepting SERS technique as a general quantitative analytical tool always has been hindered due to SERS active substrates or methods without stability or reproducibility; consequently, it is difficult to reproduce the absolute intensity of signals, even from the same samples. The two major parameters defining the quantitative performance of SERS are sensitivity and reproducibility. Therefore, the most important aspects of operating an effective SERS quantitative experiment are to prepare the SERS-active substrate or develop new SERS-based methods with stability or reproducibility. Many attempts have been carried out to realize SERS quantitative analysis for analytes. For example, the approach of self-assembly nanostructure particle or nanorod as uniform SERS substrate has been developed by several groups. Self-organized 2-dimensional (2D) close-packed arrays of different sizes (Au NPs) encapsulated by the traditional surfactant cetyltrimethylammonium bromide (CTAB) have been fabricated [15,16]. Liu et al. [17] also provide a convenient and simple method for structuring a self-organized 2D array of gold NPs based on the capillary force in the solvent evaporation process. The 2D self-assembly nanostructure arrays have highly increased surface area, so that these methods involving assembly of the different nanostructures are promising to produce active substrates with high sensitivity and good reproducibility for SERS quantitative detection. In most of these studies, typically, five to seven points are measured and averaged to construct a linear calibration curve for quantitative analysis through collecting corresponding SERS spectra. On the other hand, the SERS imaging technique has been applied for the highly reproducible and quantitative analysis of the target molecules [18] and solution-based quantitative analytical method also has been developed [19,20]. These methods are now given by a set of much more sophisticated approaches which are based on multivariate data analysis. Moreover, Hu et al. [21] have proposed a method by fabricating flexible gold nanorod arrays that can form hot spots in solution and identify the probe molecule. In previous study, we expanded the above method proposed by Hu et al. and have developed a method called metastable state surface-enhanced Raman spectroscopy (dynamic-SERS) [22–26]. This approach is very simple and reliable. Typically, a droplet of 5 μL solution is added onto the silica. The time-resolved Raman spectra are immediately recorded until the droplet is dried. The Raman spectra are recorded continuously at an interval of 12 s. About 50 spectra are recorded before the signals keep stable except huge background noise. All the successive spectra have been put together to reflect the dynamics of method. During the acquisition process (in the meantime the evaporation of water occurred), the SERS signals of analyte gradually increase and achieve the strongest value at the 25th spectrum (~300 s). Subsequently, the signals suddenly decrease and remain stable after the water evaporation is completed. Importantly, the solvent can protect the target molecules and SERS substrate from laser damage during the acquisition process; therefore, the obtained SERS spectra would reflect the real fingerprint vibrational spectra of target molecules.

On the basis of strategy of dynamic-SERS, in this study, we observed that the strongest value (a special fluctuation) during the acquisition process could be useful to monitor the relationship between absolute Raman intensity and corresponding concentration and then the dynamic-SERS was applied to quantitative detection of analytes. Also, we believe this approach would provide bright future for quantitative analysis of SERS. Herein, we presented the ability to use the dynamic-SERS as a quantitative analytical method for trace detection of pesticides. Different sources that can give rise to higher enhancements or show much better correlations between concentration and intensity will be discussed in the paper. In addition, the dynamic-SERS based quantitative analytical method by using single PS/Ag nnaoparticle as the SERS substrate has demonstrated the good performance and is capable of realizing quantitative detection of real samples.

2. Experimental section

2.1. Materials

Silver nitrate ($AgNO_3$), Crystal Violet (CV), paraoxon, sumithion, styrene, azodiisobutyronitrile (AIBN), polyvinylpyrrolidone (PVP, MW=24,000), $NaBH_4$, cetyltrimethylammonium bromide (CTAB), ascorbic acid and glycine were purchased from Sinopharm Chemical Reagent Co., Ltd. (Shanghai, China). All the chemicals were of analytical grade or better and used without further purification.

2.2. Synthesis of polystyrene (PS) particles

Typically, PVP (0.455 g) was dissolved in ethyl alcohol (100 mL) with N_2 (g) protection and then this mixture solution was heated to 70 °C. AIBN (0.0096 g) dissolved in styrene (10 mL) was slowly added to the above solution with stirring at 70 °C for 12 h. The warm reaction mixture was allowed to cool slowly to room temperature. The solution was centrifuged, and then precipitate was washed with water and re-dispersed in 10 mL water.

2.3. Synthesis of SERS substrates PS/Ag nanoparticles

PS–Ag particles were synthesized by a three-step procedure [27,28] as follows: (1) $AgNO_3$ (100 μL, 0.2 M) was added to PS solution (10 mL) and the resulting solution was vigorously stirred at 25 °C for 30 min, allowing a homogeneous diffusion of Ag^+ on the PS particles. $NaBH_4$ (300 μL, 10 mM) was added to promote the nucleation of silver NPs. This formed Ag seeds coated on PS particles. (2) The in situ growth of Ag nanoparticles on PS was achieved by adding a mixture composed of CTAB (2.5 mL, 0.2 M), glycine (2.5 mL, 0.4 mM, pH 9.5) and $AgNO_3$ (800 μL, 0.25 mM) to 10 mL PS/Ag seeds solution prepared previously. (3) Finally, ascorbic acid (600 μL, 100 mM) was added into the solution in step 2 under vigorous magnetic stirring and then the mixture was maintained at 27 °C for 30 min, followed by centrifugation (9000 rpm, 10 min) to remove excess ascorbic acid, and re-dispersed in water.

2.4. SERS measurements

All glass (silica) slides were thoroughly cleaned with aqua regia, followed by rigorous washing with plentiful ultrapure water and air-drying at 100 °C in an oven. Typically, a droplet of 5 μL analyte solution (analytes were dissolved in water) was added on PS/Ag substrates (the PS/Ag substrates have been dropped onto a clean glass slide before adding the analyte solution). The time-resolved Raman spectra were immediately recorded with 532 nm Ar^+ laser line with 10 mW power at the sample and 50 × objective. Raman spectra were continuously collected with the auto repeat function until the droplet was dried. If not explicitly stated, the exposure time and the accumulation number are 2 s and 5, respectively, the aperture is 100 μm slit, and SERS spectra region is 50–3000 cm^{-1}. All the analytes were tested according to the procedure presented here.

2.5. Time-resolved SERS spectra for pesticides

Typically, the concentrated PS/Ag substrates were dropped onto the glass slides, and then dried at room temperature. A droplet of 5 μL different concentration of pesticides solution was added on the dry PS/Ag substrates prepared previously. If not explicitly stated, the time-resolved Raman spectra were immediately recorded and analytes spectra region was 500–1800 cm^{-1}. The acquisition process generally lasted ~600 s. In the acquisition process, the SERS signals of analyte gradually increased and achieved the strongest value at the 25th spectrum (~300 s). Finally, the strongest value and corresponding concentration were observed and summarized.

2.6. Characterization and instruments

UV–vis absorption spectra were recorded using a Shimadzu UV-2550 spectrophotometer (Japan). SEM images were acquired with field-emission scanning microscopy (FE-SEM, Siron 200) at an accelerating voltage of 10 kV. SERS measurements were performed with a Raman confocal microscopy spectrometer (LabRAM HR, HORIBA Scientific, Japan). The real sample was filtered with a SHZ-D (III) water-ring vacuum pump (YUHUA).

3. Discussion and results

We prepared the polystyrene (PS) particles according to previous reports [29,30]. The representative SEM images of PS particles with better uniformity are shown in Fig. 1(A). This method yields particles with an average size of 500 nm. The growth of Ag NPs on PS particles was achieved by using a seed-mediated growth method. Silver seeds were generated on PS particles by the adsorption of silver ions followed by fast in situ reduction using sodium borohydride [27]. These Ag NPs are not particularly efficient as SERS substrates due to the small size and low level of plasmon coupling. Thus, an additional growth step was carried out by adding silver ions solution and a mixture solution of CTAB and glycine to promote the epitaxial deposition of Ag NPs on preformed seeds. SEM images of PS/Ag nanoparticles with different magnifications are shown in Fig. 1(B) and (C). Ag NPs coated on PS particles were present in the range of 35–40 nm. Fig. 1(D) exhibits the localized surface plasmon resonance (LSPR) band of PS/Ag nanoparticles, with a maximum centered at 432 nm. Also, the UV–vis absorption spectrum showed a narrow absorption band indicating substrates with highly monodisperse morphology.

Crystal Violet (CV), one of the widely used standard probes for evaluating SERS performance [31], was chosen to observe the SERS activity of PS/Ag nanoparticles. Fig. 2(A) shows the optical photographs of the isolated individual aggregates on the glass slide obtained using the visible objective of the microscopy coupled to a Raman instrument. The individual particle can be clearly identified on the glass slide. In addition, it is worthy noting that all the SERS spectra in this study were collected with these individual PS/Ag nanoparticles. To ascertain the experimental results and repeatability of substrate, the random 5 point (5 random PS/Ag nanoparticles) experiment datum was collected using the traditional SERS method. As shown in Fig. 2(B), it corresponds to the point spectrum collected randomly and the spectra indicate that the PS/Ag nanoparticle substrate basically has a good replication across the entire experiment. Meanwhile, at these 5 specific points (PS/Ag nanoparticles), the measured SERS intensity (CV – 1620 cm^{-1}) was about 8800 intensity under the traditional dry state SERS detection. Surprisingly, when a drop of 10 μL ethanol solution was

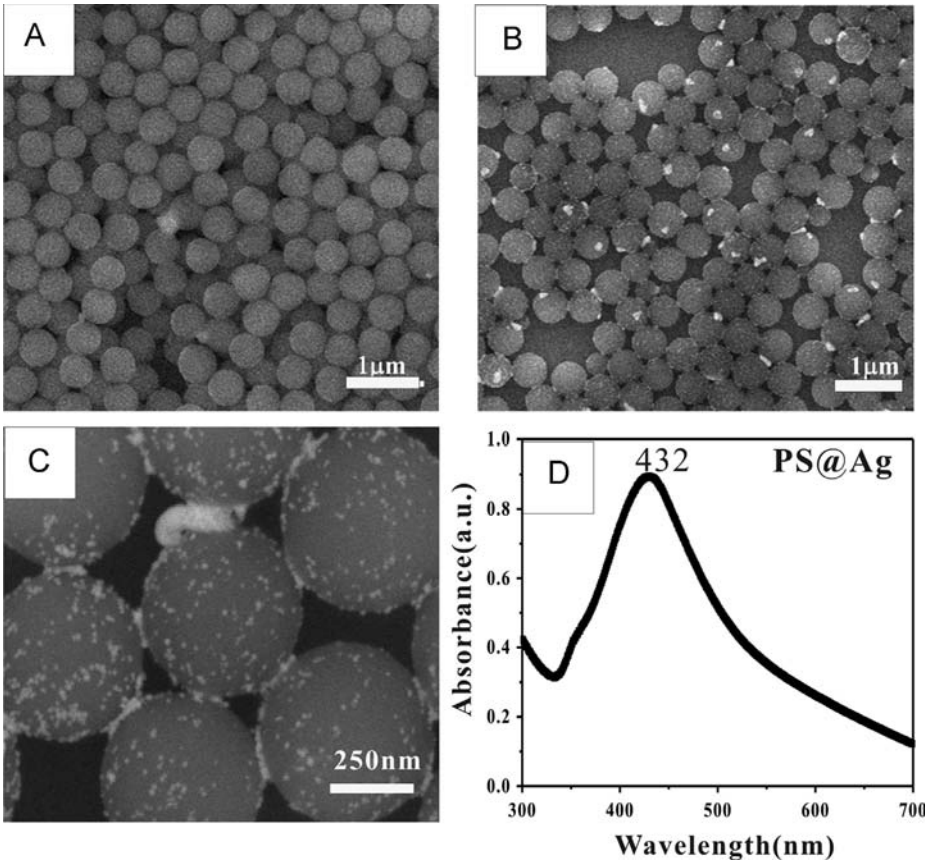

Fig. 1. (A) SEM images of PS particles. (B, C) SEM images of the final SERS substrate PS/Ag nanoparticles. (D) UV–vis spectra of PS/Ag nanoparticles.

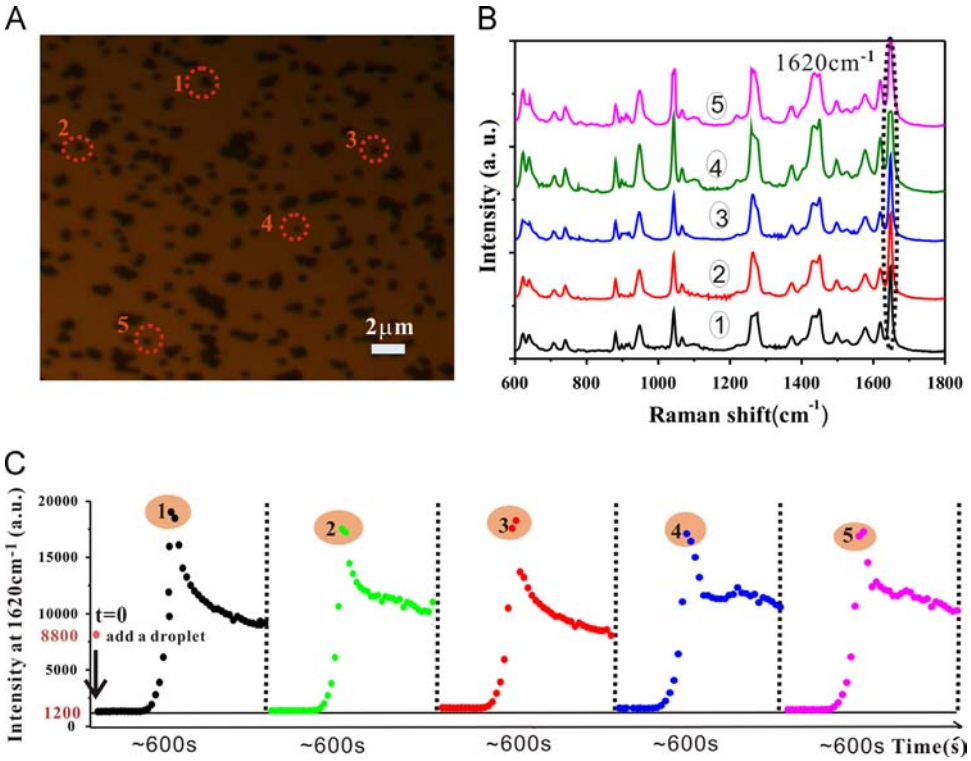

Fig. 2. (A) Optical photograph of PS/Ag nanoparticles under the visible objective of the microscopy coupled to Raman instrument with a 50× objective. Each circle spot represents a single nanoparticle. (B) SERS spectra of CV (10^{-7} M) using PS/Ag nanoparticles as the substrate with the traditional method (dry state). (C) The corresponding time-resolved SERS intensity of band 1620 cm^{-1} on point (No.1) with 5 cycles.

added onto number one point (No.1), the SERS signal of band 1620 cm^{-1}sharply decreased to 1200 intensity from 8800 intensity, possibly because the large amount of liquid had induced changes in the refractive index and also altered the path of the scattered light (Fig. 2C) [22,23,26]. Interestingly, the weak SERS signals of band 1620 cm^{-1} gradually increased in the meantime of ethanol evaporation and achieved the strongest value after ~300 s. Here, we repeated the above process with only 10 μL ethanol for five cycles at the same point (No.1). It was surprising that the Raman signals of band 1620 cm^{-1} were substantially enhanced in comparison to 8800 intensity (dry state). On the other hand, this method also can be used as an ultra-sensitive analytical technique. After 5 cycles, the intensity value at 1620 cm^{-1} reduced about 10–15%. In view of these results, we deduce that this dynamic-SERS based method with better reproducibility and weak decay would provide a possibility for quantitative analysis through monitoring the strongest absolute value and corresponding concentrations. Based on the sensitivity and reproducibility, we carried out a range of quantitative analysis experiment for target pesticides.

To evaluate the capability of dynamic-SERS method for quantitative analysis, we observed a series of alternations between the strongest values (a special fluctuation) and the concentrations. This method was based on the strategy that nanoparticles could provide several “hot spots” due to intensifying solvent volatilization and molecules collision with substrates, and also the whole volatilization process typically took less than 10 min. As reported in the previous study, SERS signals of analyte gradually increased and achieved the strongest value at ~300 s; subsequently, the signals suddenly decreased and remained stable after the water evaporation was completed. In the dynamic-SERS experiment of standard probes of CV, linear calibration curve was drawn by monitoring the value of 1620 cm^{-1} band. As shown in Fig. 3, with decreasing concentrations, the strongest value of 1620 cm^{-1} band decreases steadily from 20,000 to 2500 intensity. On the other hand, with the evolving time and intensifying volatilization process for one spectrum, the intensity value of band 1620 cm^{-1} steadily increased and achieved the strongest value at ~300 s; subsequently the signals suddenly decreased and remained stable. It is well known that, in principle there is a quantitative relationship between Raman intensity values and concentrations. However, instrument factors without unified accurate alignment, SERS substrates without better sensitivity and reproducibility and method itself ignoring variation of laser power at samples mean that it is difficult to reproduce the absolute intensity of signals, even from the same samples. These factors possibly lower 0.5–1 orders of magnitude the signals of analytes. And also other methods for quantitative analysis contain some complex process. In our study, during the process of signals gradually increasing and remaining stable, the strongest values can be chosen to monitor the relationship between intensities and concentrations. And also this dynamic-SERS method finally presents the better quantitative analysis for target analytes.

Using the dynamic-SERS analytical method, we obtained the SERS spectra of different concentrations of CV and the calibration curve. The main Raman bands of CV [31] include 1620 cm^{-1} assigned to υ(C–C) band, 1539 cm^{-1} to $\delta_s(CH_3)$ coupled with γ(C–N) band, 1443 cm^{-1} to $\delta_s(CH_3)$, 1391 cm^{-1} to $\delta_s(CH_3)$ coupled with δ(C–N), 1362 cm^{-1} to δ_{as}(C–C), 1298 cm^{-1} to υ_{as}(C–C) coupled with δ(C–H), 1171 cm^{-1} to υ(C–C) coupled with $\rho(CH_3)$, 938 cm^{-1} to ρ(CH3) coupled with γ(C–N), and 722 cm^{-1} to υ (C–C). As shown in Fig. 4(A), the spectra of signals from gradually increased to achieved the strongest value have been collected. Fig. 4(B) displays the linear calibration curve constructed by monitoring the strongest value (~300 s) of band 1620 cm^{-1} during the collecting process as a function of analyte concentration. The monitored band at 1620 cm^{-1} υ(C–C) assigned to υ(C–C) stretching was chosen as the calibration band because of its strong

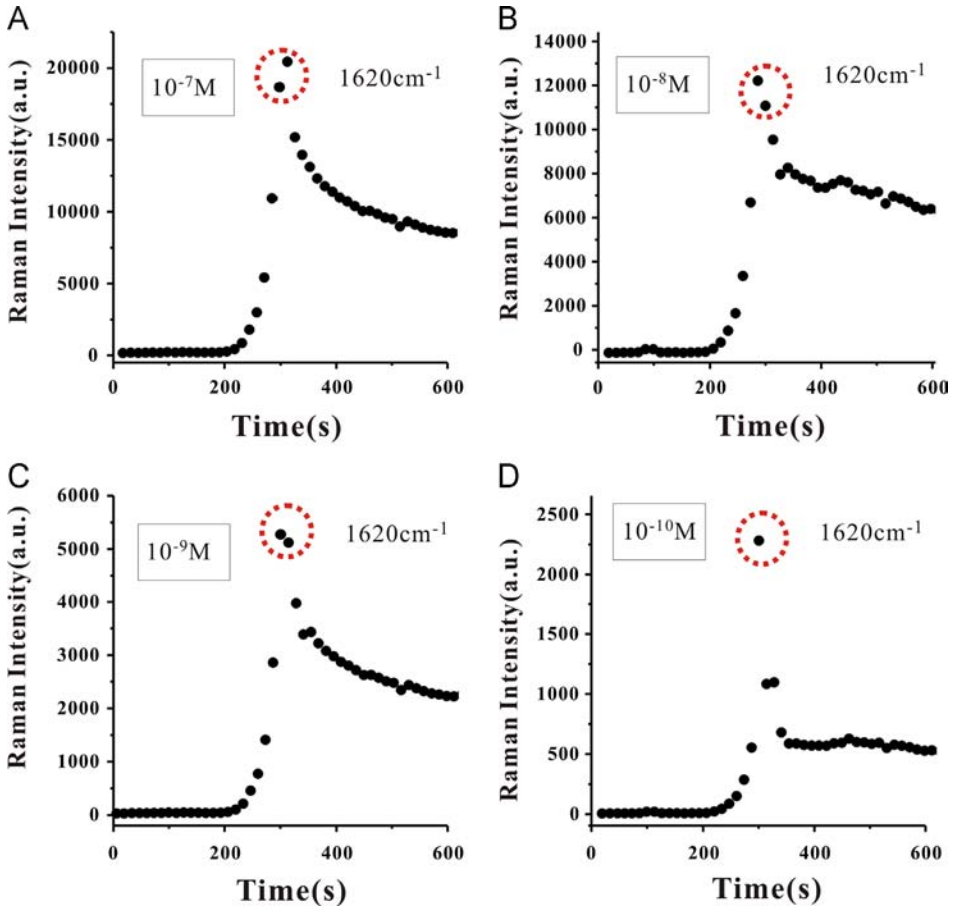

Fig. 3. Time-resolved SERS spectra of CV – 1620 cm^{-1} at different concentrations: (A) 10^{-7} M, (B) 10^{-8} M, (C) 10^{-9} M, (D) 10^{-10} M with dropping the mixture of 0.5 μL CV on the PS/Ag substrate of the silica slide at the interval of 12 s.

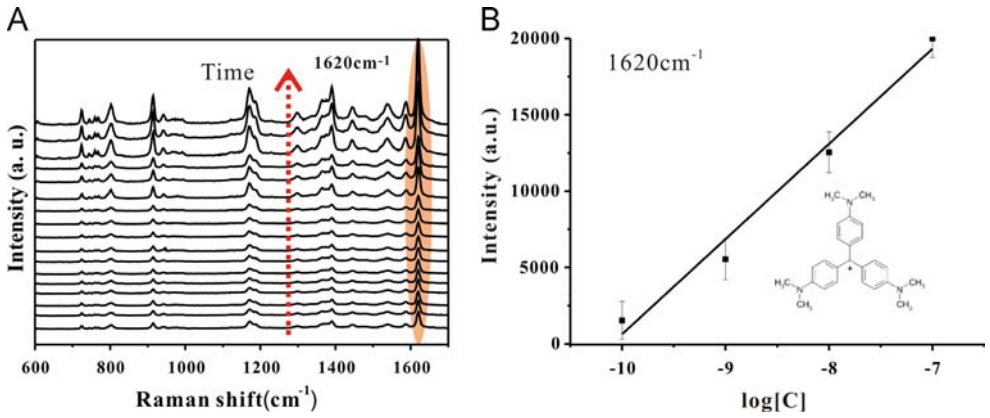

Fig. 4. (A) A part of dynamic-SERS process for continuous collecting spectra of CV – 1620 cm^{-1} from gradually increasing to the strongest intensity and (B) SERS calibration curve of the strongest intensity (1620 cm^{-1}) as a function of the CV concentration obtained by using single PS/Ag nanoparticles as substrate.

intensity with lower SNR (Signal to Noise Ratio). The error bars were the standard deviation for three independent SERS measurements and displayed a correlation coefficient R^2= 0.9899. The detection of CV exhibited a better linear calibration curve. We believe that the dynamic-SERS method will become a powerful analytical tool, so that it can be applied in many analytical fields. Also, it will provide a basic safety estimate for residual organophosphorus pesticides in lake water on the basis of above linear calibration curve.

Organic phosphorus pesticides have a sulfide bond with high toxicity. It is known that there is strong adsorption upon exposure to Au (Ag) nanoparticles. The major focus of this research was to present the dynamic-SERS method for the investigation and detection of two organic phosphorus pesticides. Different concentrations of pesticides were added to PS/Ag nnaoparticles and the SERS spectra were obtained from three independent SERS measurements for different concentrations of pesticides. The main Raman bands of paraoxon [32] included the aromatic ring (C═C) stretching at 1576 cm^{-1}, the symmetry stretching NO_2 at 1326 cm^{-1}, the aromatic ring (C–O) stretching at 1258 cm^{-1}, the C–H band (in plane)/NO_2 asymmetric stretching at 1110 cm^{-1}, the aromatic–NO_2 scissor at 869 cm^{-1} and the C–C bending at 645 cm^{-1}. Fig. 5(A) shows the part of SERS spectra alternations of paraoxon (600 nM) from gradually increased to achieved the

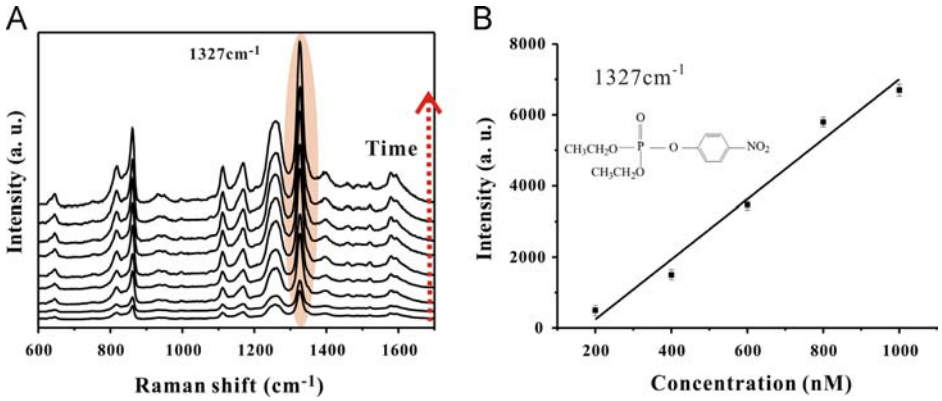

Fig. 5. (A) A part of dynamic-SERS process for continuous collecting spectra of paraoxon (600 nM) and (B) SERS linear calibration curve of the strongest intensity (1327 cm^{-1}) obtained by using PS/Ag nanoparticles as substrate.

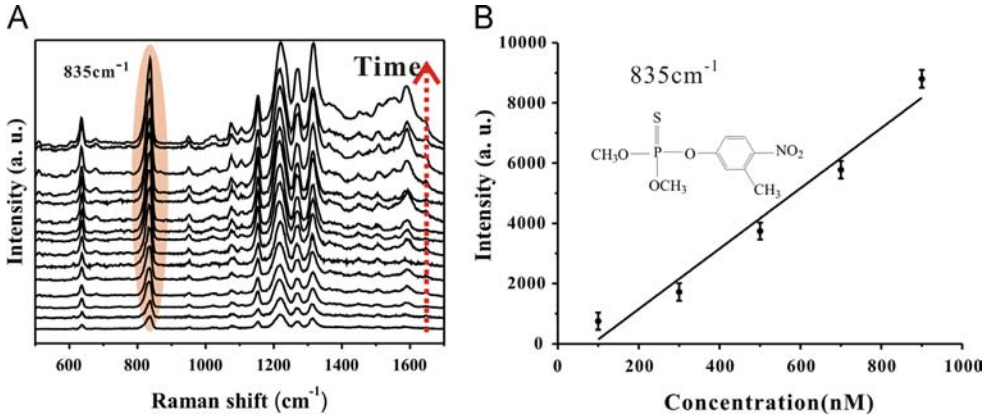

Fig. 6. (A) A part of dynamic-SERS process for continuous collecting spectra of sumithion (600 nM) and (B) SERS linear calibration curve of the strongest intensity (835 cm^{-1}) obtained by using PS/Ag nanoparticles as dynamic-SERS substrate.

strongest value. The linear calibration curve in Fig. 5(B) is constructed by monitoring the strongest value (~300 s) of band at 1327 cm^{-1} as a function of analyte concentration. The monitored band at 1327 cm^{-1} from υ(C–C) coupled with NO_2 stretching was chosen as the calibration band due to its lower SNR. It can be seen from the linear calibration curve that the SERS measurements are reproducible and the limit of detection obtained for paraoxon is approximately 96 nM. Similarly, the main Raman bands of sumithion [33] included the aromatic ring (C═C) stretch at 1595 cm^{-1}, the symmetry stretching NO_2 at 1316 cm^{-1}, the aromatic –NO_2 scissor coupled with P═S at 838 cm^{-1} and the P–S bending at 636 cm^{-1}, 1218 cm^{-1} assigned to C═S, and aromatic ring (C–N) stretch at 1076 cm^{-1}. Fig. 6(A) demonstrates the part of continuous alternations spectra of sumithion (600 nM) during the collecting process. The linear calibration curve constructed by monitoring the strongest value of band 835 cm^{-1} as a function of analyte concentration has been shown in Fig. 6(B). The error bars exhibited the standard deviation of the strongest Raman intensity (~300 s) obtained from three independent SERS measurements. It can be seen that the SERS measurements are also reproducible and the limit of detection obtained for sumithion is approximately 34 nM. Above results further indicate that this is a method that can construct a linear calibration curve with a high correlation coefficient through monitoring the strongest SERS intensity as a function of corresponding concentration.

Table 1 displays calculated limits of detection, limits of quantitation, the correlation coefficient (R^2) for each linear calibration curve. Limits of detection are calculated by determining the minimum distinguishable signal using the following expression [19]:

$$S_m = \overline{S_{bl}} + ks_{bl}$$

where S_m is the minimum distinguishable signal (the signal is from the special fluctuation), S_{bl} is the Raman signal generated by a blank measurement of the PS/Ag substrate in the absence of bands 1327 cm^{-1} and 835 cm^{-1}. κ is the proportionality constant, and s_{bl} is the standard deviation of κ blank measurements. In the case of the limit of detection, the κ value is 3, and in the case of the limit of quantitation, the κ value is 10. The limits of detection are determined by substituting the minimum distinguishable signal to fit equation of the linear calibration curve. The differences of limits detection between two pesticides indicated in Table 1 should be attributed to the differences of interaction strength between the pesticide and SERS substrate.

Table 1
Analytical figures of merit for quantitative SERS detection of paraoxon and sumithion.

Pesticides	R^2	Limit of detection (nM)	Limit of quantitation (nM)
Paraoxon	0.9879	96	152
Sumithion	0.9898	34	57

On the basis of linear calibration curve, the tests of real samples were applied to different matrices, including deionized (DI) water, real lake water and rice water. The real lake water was collected from

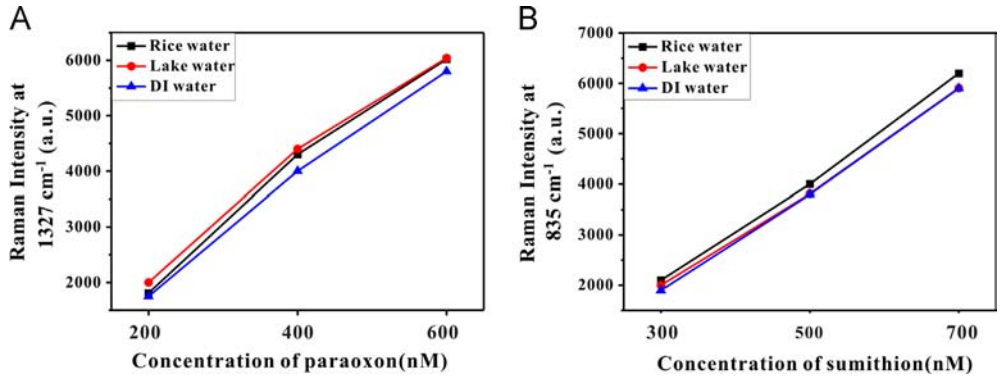

Fig. 7. (A) The strongest intensities of SERS signals at 1379 cm^{-1} (paraoxon) and (B) at 835 cm^{-1} (sumithion) as a function of the concentrations spiked in different matrices of natural lake water, rice water and DI water. These spectra are collected at the strongest value (25th spectrum, ~300 s) during the acquisition process.

a local lake and the rice water was bought from a local market. All samples were filtered through 0.22 μm aperture of membrane under the water-ring vacuum pump to remove any particulate suspension prior to the preparation of spiked solutions with different concentrations of analytes. For the dynamic-SERS experiment, 5 μL of the spiked sample solution was dropped onto the PS/Ag substrate and then the time-resolved spectra were collected immediately. These spectra were obtained at the strongest value (25th spectrum, ~300 s) during the acquisition process. As shown in Figs. S1 and S2, the fingerprint SERS signals of paraoxon and sumithion could be observed clearly from DI water, real lake water and rice water, although the background noises were different. Fig. 7 shows the comparison of the strongest SERS intensities at 1327 cm^{-1} and 835 cm^{-1} obtained from each matrix. The SERS signals of pesticides in lake water and rice water were slightly higher than those of pesticides in DI water. Above result reported that the impurities in lake water and rice water had slight 3.5% interferences on the SERS signals of the analytes compared to those of DI water. For the selectivity of this dynamic-SERS method, different target molecules indicated different fingerprint information which combined with the structure of analytes to distinguish analytes. On the other hand, when the sample contained more than two targets, the analyte which presented the SERS signals should attribute to the high affinity of the compound to the surface of the PS/Ag substrate.

4. Conclusions

We demonstrated the simple dynamic-SERS method for sensitive and quantitative detection of pesticides by using PS/Ag nanoparticles as the substrate. PS/Ag can provide several "hot spots" due to intensifying solvent volatilization and the drastic collision of molecules with substrates and this method is highly sensitive with limit of detection in the low 10 nM range for two pesticides. Meanwhile, a single particle as the SERS-active substrate is easily located by optical microscopy for the collection of SERS spectra. Importantly, this method shows much better correlations between concentration and intensity, and based on the linear calibration curve, the tests of real samples are applied to different matrices with slight interference. We hope that this approach would provide bright future for quantitative analysis of SERS.

Acknowledgments

This work was supported by Major national scientific instrument and equipment development project (2011YQ0301241001 and 2011YQ0301241101).

Appendix A. Supporting information

Supplementary data associated with this article can be found in the online version at http://dx.doi.org/10.1016/j.talanta.2014.03.075.

References

[1] K. Vandecasteele, I. Gaus, W. Debreuck, K. Walraevens, Anal. Chem. 72 (2000) 3093–3101.
[2] D. Li, D.W. Li, J.S. Fossey, Y.T. Long, Anal. Chem. 82 (2010) 9299–9305.
[3] D. Li, L. Qu, W. Zhai, J. Xue, J.S. Fossey, Y. Long, Environ. Sci. Technol. 45 (2011) 4046–4052.
[4] J. Dong, Q. Chen, C. Rong, D. Li, Y. Rao, Anal. Chem. 83 (2011) 6191–6195.
[5] A. Rumyantseva, S. Kostcheev, P.M. Adam, S.V. Gaponenko, S.V. Vaschenko, O.S. Kulakovich, A.A. Ramanenka, D.V. Guzatov, D. Korbutyak, V. Dzhagan, A. Stroyuk, V. Shvalagin, ACS Nano 7 (2013) 3420–3426.
[6] S.M. Adams, S. Campione, F. Capolino, R. Ragan, Langmuir 29 (2013) 4242–4251.
[7] D.W. Li, L.J. Pan, S. Li, K. Liu, S.F. Wu, W. Peng, J. Phys. Chem. C 117 (2013) 6861–6871.
[8] P.B. Liu, Y. Huang, L. Wang, Mater. Lett. 97 (2013) 173–176.
[9] K. Lee, J. Irudayaraj, Small 9 (2013) 1106–1115.
[10] L. Wei, C. Liu, B. Chen, P. Zhou, H.C. Li, L.H. Xiao, E.S. Yeung, Anal. Chem. 85 (2013) 3789–3793.
[11] T. Yajima, Y.Y. Yu, M. Futamata, J. Raman. Spectrosc. 44 (2013) 406–411.
[12] T. Bocklitz, A. Walter, K. Hartmann, P. Rosch, J. Popp, Anal. Chim. Acta 704 (2011) 47–56.
[13] P.H.B. Aoki, E.G.E. Carreon, D. Volpati, M.H. Shimabukuro, C.J.L. Constantino, R.F. Aroca, O.N. Oliveira, F.V. Paulovich, Appl. Spectrosc. 67 (2013) 563–569.
[14] K.A. Hollywood, I.T. Shadi, R. Goodacre, J. Phys. Chem. C 114 (2010) 7308–7313.
[15] H. Wang, C.S. Levin, N.J. Halas, J. Am. Chem. Soc. 127 (2005) 14992–14993.
[16] A. Wei, Chem. Commun. 15 (2006) 1581–1591.
[17] S.T. Liu, T. Zhu, R.S. Hu, Z.F. Liu, Phys. Chem. Chem. Phys. 4 (2002) 6059–6062.
[18] M. Lee, S. Lee, J.H. Lee, H.W. Lim, G.H. Seong, E.K. Lee, S.I. Chang, C.H. Oh, J. Choo, Biosens. Bioelectron. 26 (2011) 2135–2141.
[19] B. Saute, R. Narayanan, Analyst 136 (2011) 527–532.
[20] B. Saute, R. Premasiri, L. Ziegler, R. Narayanan, Analyst 137 (2012) 5082–5087.
[21] F.S.O. Min Hu, W. Wu, I. Naumov, X.M. Li, A.M. Bratkovsky, Z.L.R. Stanley Williams, J. Am. Chem. Soc. 132 (2010) 12820–12822.
[22] K. Qian, L.B. Yang, Z.Y. Li, J.H. Liu, J. Raman Spectrosc. 44 (2013) 21–28.
[23] H.L. Liu, Y.D. Sun, Z. Jin, L.B. Yang, J.H. Liu, Chem. Sci. 4 (2013) 3490–3496.
[24] P. Li, H.L Liu, L.B. Yang, J.H. Liu, Talanta 117 (2013) 39–44.
[25] L.B. Yang, H.L. Liu, Y.M. Ma, J.H. Liu, Analyst 137 (2012) 1547–1549.
[26] L.B. Yang, H.L. Liu, J. Wang, F. Zhou, Z.Q Tian, J.H. Liu, Chem. Commun. 47 (2011) 3583.
[27] R. Contreras-Caceres, S. Abade-Cela, P. Guardia-Giros, A. Fernandez-Barbero, J. Perez-Juste, R.A. Alvarez-Puebla, L.M. Liz-Marzan, Langmuir 27 (2011) 4520–4525.
[28] Z.S. Yang, Y.W. Lin, W.L. Tseng, H.T. Chang, J. Mater. Chem. 15 (2005) 2450–2454.
[29] C. Yuen, W. Zheng, Z.W. Huang, J. Raman Spectrosc. 41 (2010) 374–380.
[30] H.H. Lin, J. Mock, D. Smith, T. Gao, M.J. Sailor, J. Phys. Chem. B 108 (2004) 11654–11659.
[31] C.C. Maria Vega Can~amares, Ronald L. Birke, John R. Lombardi, J. Phys. Chem. C 112 (2008) 20295–20300.
[32] F. Fathi, F. Lagugne-Labarthet, D.B. Pedersen, H.B. Kraatz, Analyst 137 (2012) 4448–4453.
[33] O.I. Guliy, O.V. Ignatov, S.Y. Shchyogolev, V.D. Bunin, V.V. Ignatov, Anal. Chim. Acta 462 (2002) 165–177.